Stabilizing Bolaform Amphiphile Interfacial Assemblies by Introducing Mesogenic Groups

Mingfeng Wang, Dengli Qiu, Bo Zou, Tao Wu, and Xi Zhang*[a]

Abstract: We describe the synthesis and characterization of the mesogen-bearing bolaform amphiphile 4,4′-dihydroxybiphenylbis(11-pyridinium-*N*-yl-undecanoic ester) dibromide (BP-10) and its solid/liquid interfacial self-assembly. Cylindrical micelles are directly observed by atomic force microscopy (AFM) at the interface between mica and the aqueous solution above the critical micelle concentration (cmc). In situ and ex situ AFM studies indicate that the cylindrical micelles are stable both at the mica/solution interface and in the dry state. The enhanced stability of the micellar structures enables a detailed investigation of their self-assembly behavior and supramolecular structures at the interface. The adsorption model proposed here is supported by the variation of the interfacial self-assemblies on changing the solution concentration and substrate temperature.

Keywords: amphiphiles · micelles · self-assembly · supramolecular chemistry

Introduction

Supramolecular self-assembly confined to interfaces has attracted increasing interest from chemists, physicists, and biologists.[1, 2] Conventional surfactants such as hexadecyltrimethylammonium bromide (CTAB) can form adsorbed spherical, cylindrical, or hemicylindrical micelles as well as bilayer structures at the solid/liquid interface.[3–6] Such self-assembled structures are labile, however, and can be easily influenced by the external environment, which prevents the thorough identification of the supramolecular structures of the interfacial micelles.[6] Both basic research and applications in materials science require the design and synthesis of building blocks suitable for constructing stable supramolecular assemblies.

A stable supramolecular assembly requires a strong association among its assembling units through different forms of intermolecular forces. The amphiphilic lipid assemblies can be made more rigid by using noncovalent approaches that lead to hydrogen bonding or an increase of the van der Waals interaction through $\pi-\pi$ stacking. The assembly can also be strengthened by covalent modifications such as surface cross-linking, coating, and internal polymerization.[7] We have focused on the confined supramolecular nanostructures of mesogen-bearing amphiphiles at the solid/liquid interface.[8] By introducing mesogenic groups into amphiphiles, we obtained stable nanostructures with different morphologies at the mica/solution interface.

Here we present the synthesis and characterization of a bolaform amphiphile (BP-10) that contains a cationic pyridinium head group at each end of the alkyl chain and a biphenyl mesogenic unit. The structures of the assemblies at the interface were investigated by means of in situ and ex situ atomic force microscopy (AFM). We anticipate that the increased stability of the adsorbed micelles by the introduction of the mesogenic unit will enable detailed studies of their supramolecular structures and interfacial behavior. Knowledge of the interfacial self-assembly of amphiphiles is important not only for better understanding of self-assembly but also for potential applications in materials science, such as the template synthesis of functional nanomaterials, and surface patterning on the nanometer scale.

Results and Discussion

Design, synthesis, and self-organization in solution: Bolaform amphiphiles are molecules that contain two hydrophilic moieties connected by a hydrophobic chain.[9] The synthetic route to the mesogen-bearing bolaform amphiphile BP-10 is shown in Scheme 1. Both the mesogenic biphenyl group and the long flexible hydrocarbon-chain spacer may enhance the intermolecular interaction among the amphiphiles and allow a more stable supramolecular organization.

The dependence of the conductivity of the solution on concentration of BP-10 is shown in Figure 1. The plot shows

[a] Prof. Dr. X. Zhang, M. Wang, D. Qiu, Dr. B. Zou, T. Wu
Key Lab of Supramolecular Structure & Materials
College of Chemistry, Jilin University
Changchun 130023 (P. R. China)
Fax:(+86) 431-8980729
E-mail: xi@jlu.edu.cn

© 2003 WILEY-VCH Verlag GmbH & Co. KGaA, Weinheim
0947-6539/03/0908-1876 $ 20.00+.50/0 *Chem. Eur. J.* **2003**, *9*, No. 8

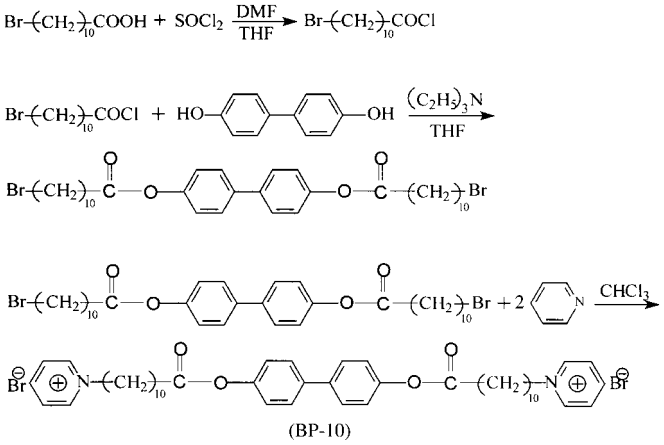

Scheme 1. Synthesis of BP-10.

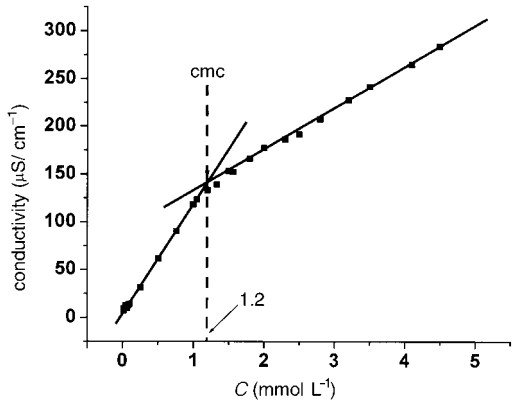

Figure 1. Dependence of the solution conductivity of BP-10 on concentration; the cmc is 1.2×10^{-3} M.

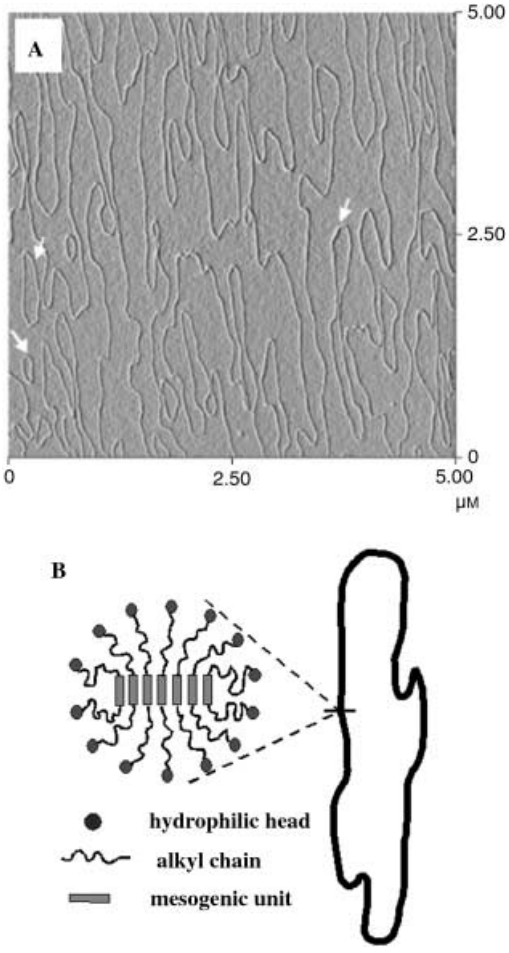

Figure 2. A) In situ AFM images (5 μm × 5 μm) of BP-10 adsorbed at the mica/solution interface. The solution concentration is 4.0×10^{-3} M ($\sim 3 \times$ cmc). The arrows indicate looplike self-closed cylindrical micelles. B) Schematic of the loop-like self-closed cylindrical micelles.

that the critical micelle concentration (cmc) occurs at 1.2×10^{-3} M; above this concentration, the amphiphiles self-organize into micelles.

The mesogen-bearing bolaform amphiphile BP-10 should tend to form various organized supramolecular structures, for example lamellar structures and cylindrical micelles, in the solution above the cmc. These possibilities are partially attributed to the molecular structure of BP-10, which comprises a single alkyl chain containing a rigid biphenyl unit and two ionic pyridinium head groups.[10]

AFM in situ and ex situ characterization of interfacial micelles: The adsorbed micelles of BP-10 were directly observed by in situ AFM at the interface between mica and a 4.0×10^{-3} M ($\sim 3 \times$ cmc) solution of BP-10. As shown in Figure 2A, BP-10 forms cylindrical micelles extending over micrometers. These micellar structures are rather monodisperse, with an average width of 40 nm as measured from the section analysis. There is no change even after prolonging the incubating time up to 24 h. Interestingly, large loops with different sizes formed, as indicated with arrows in Figure 2A. We believe the looplike assemblies are formed by the self-closure of the cylindrical micelles. Hydrophilic and hydrophobic parts of BP-10 are completely segregated in this kind of supramolecular organization (Figure 2B), suggesting that the looplike self-closed cylindrical micelles are thermodynamically more stable assemblies than the cylindrical micelles with open ends.

After the mica was incubated for 30 min in the solution with the same concentration, it was removed from the solution, immediately dip-rinsed in pure water, and then dried overnight at room temperature. Ex situ AFM reveals that the adsorbed micellar structures persist even in the dry state (Figure 3). It should be noted that the density of the adsorbed cylindrical micelles in the dry state is greater than that observed by in situ AFM, which can be attributed to the capillary forces among micelles during the solvent evaporation in the drying process. The measured width of the micellar structures with ex situ AFM is approximately 40 nm, which is almost the same as the width measured by in situ AFM. There should be some effect of the tip–sample convolution that may influence the measured width of the micellar structures. In our experiment, for the in situ AFM measurements we used a sharpened Si_3N_4 cantilever with a tip radius of about 20 nm for the tapping mode in fluid. For the ex situ AFM measurments, we used an Si cantilever with a tip radius of about 50 nm for the tapping mode in air. Comparing the AFM images obtained with these two modes, we find that tip curvature has little influence in our case.

 © 2003 WILEY-VCH Verlag GmbH & Co. KGaA, Weinheim 0947-6539/03/0908-1877 $ 20.00+.50/0

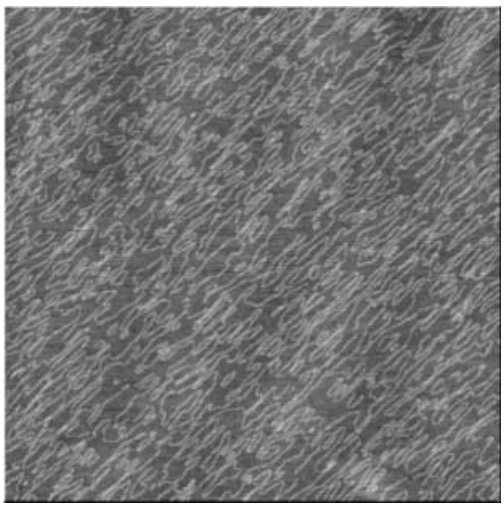

Figure 3. Ex situ AFM images (5 μm × 5 μm) of BP-10 adsorbed at the mica/solution interface. The solution concentration is 4.0×10^{-3} M (~3 × cmc). The micellar structures remained after the dip-washing and drying process, suggesting that such supramolecular self-assemblies are robust.

Usually, the micelles formed by conventional surfactants are labile at the solid/liquid interface. For example, cylindrical micelles of CTAB at the mica/solution interface can evolve into a flat bilayer sheet within 24 h. The adsorbed second layer is removed in the drying process.[6] In contrast, the adsorbed cylindrical micelles of BP-10 are stable both at the mica/solution interface and in the dry state, however, suggesting that these supramolecular assemblies are robust. Their enhanced stability can be partially attributed to the strong association within the cylindrical micelles and the strengthened intermolecular interaction due to the introduction of the mesogenic unit into the amphiphile.

Concentration effect: To substantiate the adsorption of the micellar structures, we studied the adsorption of BP-10 at different bulk solution concentrations by ex situ AFM. For a solution concentration of 2.0×10^{-4} M, far below the cmc, we observed only flat sheet structures and random domains with different diameters (Figure 4A). The section analysis gives a height of approximately 3 nm for the flat sheet structures, suggesting monolayer deposition if the tilted orientation of BP-10 adsorbed on mica is taken into consideration. For a solution concentration of 1.0×10^{-3} M, slightly lower than the cmc, the interfacial cylindrical micelles have already begun to appear (Figure 4B). This effect can be rationalized by the possibility that the concentration of BP-10 near the mica surface is higher than in the bulk because of the electrostatic surface potential.[6a] For the concentrations of 1.0×10^{-3} M and 2.0×10^{-3} M, some defects embedded in the adsorbed assemblies are always observed in addition to the cylindrical micelles (Figure 4B and C, respectively). The depth of the defects against the monolayer islands is approximately 3 nm, which also corresponds to the deposition of a monolayer of BP-10. For the concentration of 4.0×10^{-3} M, cylindrical micelles covering at least 5 μm × 5 μm without defects can be observed (Figure 3). In general, the coverage of the mica surface and the density of the cylindrical micelles both increase as the concentration increases from 1.0×10^{-3} M to 4.0×10^{-3} M.

Based on the AFM images, we conclude that there is a coadsorption of cylindrical micelles and monomers at the interface between mica and the solution above the cmc. The ratio of cylindrical micelles to monomers increases as the concentration of the solution increases; that is, the higher the concentration, the more cylindrical micelles are formed in the solution and thus adsorbed at the interface. The adsorption model proposed here is consistent with the adsorption process and mechanism of CTA^+X^- proposed by Chen et al.[4]

In situ temperature-dpendent AFM studies: To further study the stability of the micellar structures of BP-10 at the interface, we investigated the change of the interfacial assemblies on increasing the temperature of the substrate. The interfacial structural transformation was monitored by in situ temperature-dependent AFM. Figure 5A shows the dry-state structure at room temperature of BP-10 which was adsorbed from a solution of 4.0×10^{-3} M onto the mica substrate. There are some defects embedded in the adsorbed monolayer and cylindrical micelles. The width of the cylindrical micelle is approximately 40 nm (outlined by the rectangle in Figure 5A). No obvious changes are observed until the substrate is heated to 50° C. With the gradual

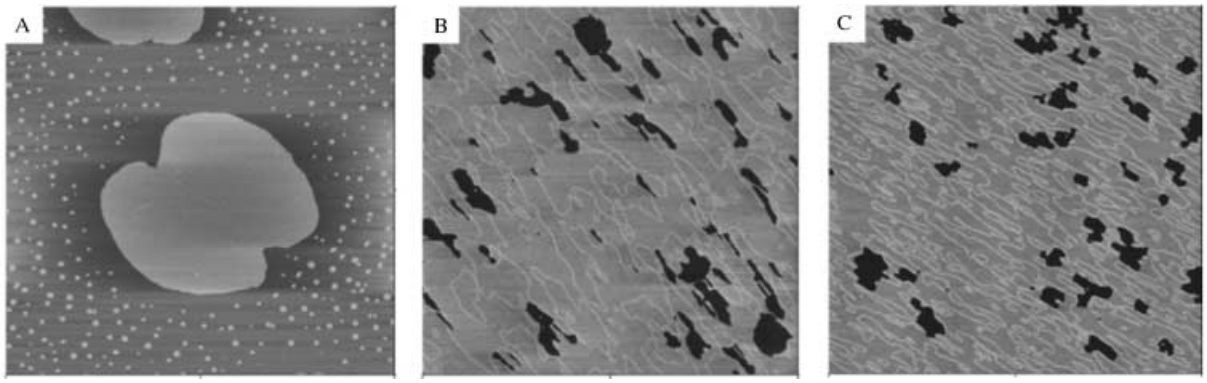

Figure 4. Ex situ AFM images of the adsorbed self-assemblies at different solution concentrations: A) 2.0×10^{-4} M; B) 1.0×10^{-3} M; C) 2.0×10^{-3} M (the image size is 5 μm × 5 μm in each case and each image is recorded in the height mode). The density of the cylindrical micelles increases as the concentration increases from 1.0×10^{-3} M to 2.0×10^{-3} M. The dark regions in B) and C) are adsorption defects, the depth of which is (3 ± 0.1) nm, corresponding to a monolayer deposition of BP-10.

© 2003 WILEY-VCH Verlag GmbH & Co. KGaA, Weinheim
0947-6539/03/0908-1878 $ 20.00+.50/0 *Chem. Eur. J.* **2003**, *9*, No. 8

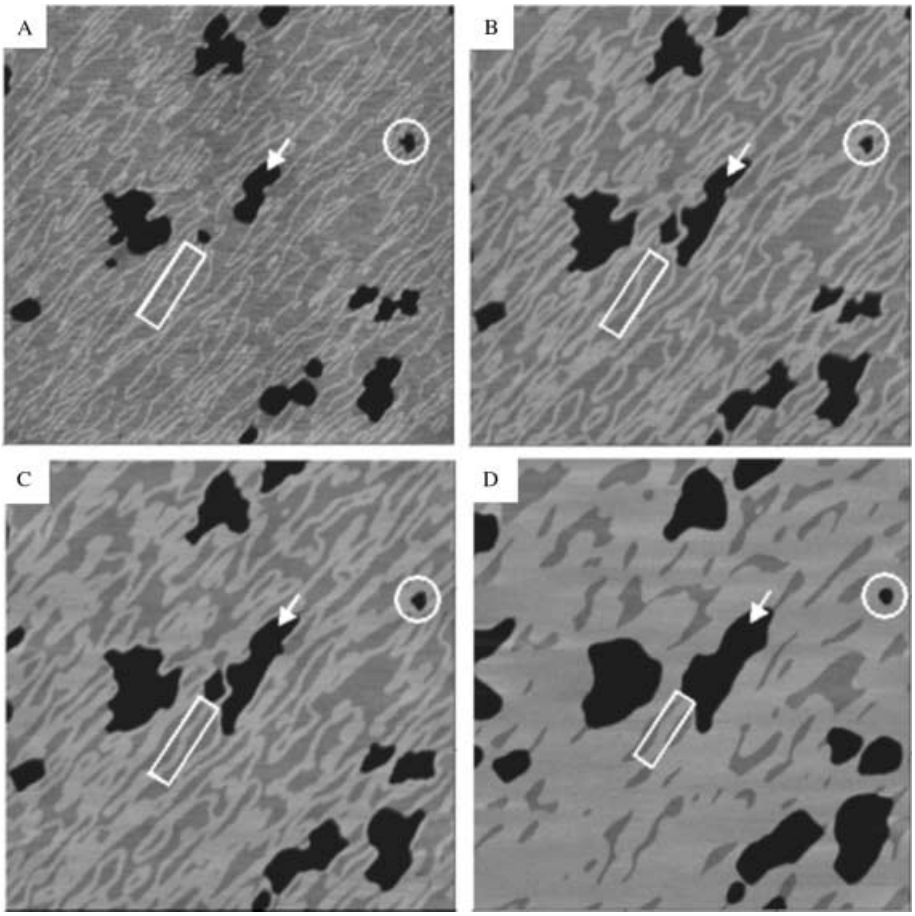

Figure 5. Ex situ AFM images showing the structural transformation of the adsorbed micellar structures on changing the substrate temperature: A) 25° C; B) 55° C; C) 59° C; D) 70° C (the image size is 3 μm × 3 μm in each case and each image is recorded in the height mode). The rectangular blocks indicate a single cylindrical micelle that becomes wider and wider on increasing the substrate temperature. The arrows indicate the defects embedded in the monolayer islands. These defects are enlarged during the heating process but do not change further after they extend over the fringes of cylindrical micelles. The circles show the defects embedded among the micellar structures. These defects change little during the heating process.

increase of the substrate temperature from 50° C, the cylindrical micelles become wider and wider. After the substrate is heated to 70° C and held at this temperature for 1 h, the single cylindrical micelle becomes as wide as 70–80 nm (see rectangle in Figure 5D). We believe these changes are the result of the lateral diffusion of the cylindrical micelles on mica, which is caused by the enhanced mobility on heating the substrate. In addition, the height difference between the white and gray regions is around 0.5 nm, which also supports the model of cylindrical micelles.

We note that the defects embedded in the monolayer islands (shown with arrows in Figure 5) are enlarged on heating the substrate. The defects do not change further after they extend over the fringes of the cylindrical micelles. But the defects embedded among the cylindrical micelles (shown as circles in Figure 5) change little during the heating process, indicating that in spite of lateral diffusion the cylindrical micelles do not collapse to the substrate to form a monolayer structure. We conclude from these results that the monolayer islands around the defects are not as stable as the cylindrical micelles. From Figure 5, it is also clearly observed that neighboring micellar structures combine to give a wider one on increasing the temperature.

Conclusion

We have synthesized a mesogen-bearing bolaform amphiphile that contains two cationic pyridinium head groups and a biphenyl mesogenic unit. By introducing the mesogenic unit into the bolaform amphiphile, we have succeeded in obtaining stable supramolecular assemblies at the mica/solution interface. In situ and ex situ AFM studies provide direct evidence for the interfacial self-assembly of cylindrical micelles and monomers. The formation of the cylindrical micelles depends on the solution concentration. For the concentrations above the cmc, the density of the cylindrical micelles increases as the concentration increases. In situ temperature-dependent AFM provides detailed information about the diffusion and integration process of the cylindrical micelles on the mica surface. Due to the stability of the cylindrical micelles, AFM has been effectively used to investigate the morphology, the supramoledular structure, and the interfacial behavior of such assemblies. The stable cylindrical micelles are also promising for use in template synthesis and assembly of further functional supramolecular structures and nanomaterials.

Experimental Section

Materials: 4,4′-Dihydroxybiphenyl (97% purity) and 11-bromoundecanoic acid (99% purity) were purchased from Aldrich. DMF, THF, and triethylamine were all distilled and dried before use.

Preparation of 11-bromoundecanoic acid chloride: A mixture of 11-bromoundecanoic acid (2.86 g, 10.8 mmol) and thionyl chloride (10 mL, 137 mmol) in THF (50 mL), and several drops of DMF as catalyst were refluxed for 4 h. When the mixture was cooled, the solvent and excess thionyl chloride were evaporated in vacuum.

Synthesis of 4,4′-dihydroxybiphenylbis(11-bromoundecanoic ester): The freshly prepared 11-bromoundecanoic acid chloride (10.8 mmol) was added dropwise to a stirred solution of 4,4′-dihydroxybiphenyl (1 g, 5.4 mmol) and triethylamine (1.6 mL) in THF (10 mL). The mixture was refluxed for 2 h and then stirred at room temperature overnight. The precipitated triethylamine–hydrochloride was filtered. The filtrate was extracted with diethyl ether. The organic layer was washed with 0.1M HCl,

saturated aqueous $NaHCO_3$, and water. After the solution had been dried with $MgSO_4$, the solvent was removed in vacuum. The crude product was purified by column chromatography (silica gel, dichloromethane) and recrystallized from 1:1 (v/v) dichloromethane/cyclohexane to obtain colorless needlelike crystals of 4,4′-dihydroxybiphenylbis(11-bromoundecanoic ester). Yield: 45 %; ^{1}HNMR (400 MHz, $CDCl_3$): $\delta = 7.56 - 7.54$ (d, 4H; Ph-H), 7.15 – 7.13 (d, 4H, Ph-H), 3.43 – 3.39 (t, 4H, Br-CH_2), 2.60 – 2.56 (t, 4H, -OCOCH_2), 1.89 – 1.84 (m, 4H; Br-CH_2CH_2), 1.81 – 1.73 (m, 4H; -OCO-CH_2CH_2), 1.56 – 1.32 ppm (m, 24H; -$CH_2CH_2(CH_2)_6CH_2CH_2$-).

Synthesis of 4,4′-dihydroxybiphenylbis(11-pyridinium-*N*-yl-undecanoic ester) dibromide (BP-10): Pyridine (6 mL, 75 mmol) was added to the stirred solution of 4,4′-dihydroxybiphenylbis(11-bromoundecanoic ester) (0.5 g, 0.73 mmol) in $CHCl_3$ (10 mL). The mixture was stirred and refluxed for 24 h (under a highly purified nitrogen atmosphere). After the mixture had been allowed to cool to room temperature, it was added dropwise to benzene (100 mL). A white solid precipitated. The crude product was redissolved in acetonitrile and precipitated twice in diethyl ether. Yield: 85 %; m.p. 167 °C; ^{1}HNMR (400 MHz, DMSO): $\delta = 9.10$ (t, 4H; Py-H), 8.62 – 8.58 (d, 2H; Py-H), 8.18 – 8.14 (t, 4H; Py-H), 7.70 – 7.68 (d, 4H; Ph-H), 7.21 – 7.19 (d, 4H; Ph-H), 4.62 – 4.58 (t, 4H; Py-CH_2), 2.61 – 2.57 (t, 4H; -OCOCH_2), 1.91 (m, 4H; Py-CH_2CH_2), 1.66 – 1.63 (m, 4H; -OCO-CH_2CH_2), 1.28 ppm (m, 24H; -$CH_2CH_2(CH_2)_6CH_2CH_2$-).

Sample preparation and AFM characterization: Muscotive mica (PLANO W. Plannet GmbH, Germany) was freshly cleaved before immersion in the aqueous solution of the amphiphile at an appropriate concentration. AFM images were recorded in situ and ex situ at the solid/liquid interface by using commercial instruments Nanoscope IIIa AFM Multimode (Digital Instrument, CA) at room temperature. Sharpened Si_3N_4 cantilevers of ~20 nm tip radius were used for the tapping mode in fluid; Si cantilevers of ~50 nm tip radius were used for the tapping mode in air. All cantilevers were purchased from Park Scientific, CA. Before the in situ AFM images were recorded, an aqueous solution of the amphiphile with an appropriate concentration was injected into the liquid cell and allowed to equilibrate for at least 1 h. The solution was held within the liquid cell by an O-ring. In situ AFM images were obtained with a tapping mode in fluid. Before the ex situ AFM images were recorded, the mica was first incubated in the aqueous solution of BP-10 for 30 min, then taken out from the solution, immediately dip-rinsed in Milli-Q water, and dried overnight at room temperature in a desiccator with P_2O_5. Ex situ AFM images were obtained with tapping mode in air. In the in situ temperature-dependent AFM experiment, the mica substrate with the adsorbed sample was glued onto a stainless steel disk and then heated in air using the temperature heater of the AFM (MultiMode). The images were captured with tapping mode in air at a desired temperature equilibrated for at least 5 min.

Acknowledgements

This project is supported by the Major State Basic Research Development Program (Grant No. G2000078102), National Natural Science Foundation of China, and a key project of Ministry of Education, P. R. China. We gratefully acknowledge F. Shi for the synthesis of the amphiphile BP-10. We also gratefully acknowledge Barbara Whitesides from Harvard University for carefully polishing the English of this paper. We also thank the one of the referees for helpful comments.

[1] S. Manne, G. G. Warr, *Supramolecular Structure in Confined Geometries*, ACS Symposium Series, *Vol. 736*, American Chemical Society: Washington, DC **1999**.
[2] S. T. Nguyen, D. L. Gin, J. H. Hupp, X. Zhang, *Proc. Natl. Acad. Sci. USA* **2001**, *98*, 11 849 – 11 850.
[3] S. Manne, H. E. Gaub, *Science* **1995**, 270, 1480 – 1482.
[4] Y. L. Chen, S. Chen, C. Frank, J. Israelachvili, *J. Colloid Interface Sci.* **1992**, *153*, 244 – 265.
[5] a) S. Manne, J. P. Cleveland, H. E. Gaub, G. D. Stucky, P. K. Hansma, *Langmuir* **1994**, *10*, 4409 – 4413; b) I. A. Aksay, M. Trau, S. Manne, I. Honma, N. Yao, L. Zhou, P. Fenter, P. M. Eisenberger, S. M. Gruner, *Science* **1996**, *273*, 892 – 898; c) S. Manne, T. E. Schäffer, Q. Huo, P. K. Hansma, D. E. Morse, G. D. Stucky, I. A. Aksay, *Langmuir* **1997**, *13*, 6382 – 6387; d) M. Jaschke, H. J. Butt, H. E. Gaub, S. Manne, *Langmuir* **1997**, *13*, 1381 – 1384; e) H. N. Patrick, G. G. Warr, S. Manne, I. A. Aksay, *Langmuir* **1999**, *15*, 1685 – 1692.
[6] a) R. E. Lamont, W. A. Ducker, *J. Am. Chem. Soc.* **1998**, *120*, 7602 – 7607; b) W. A. Ducker, E. J. Wanless, *Langmuir* **1999**, *15*, 160 – 168.
[7] a) J. Song, Q. Cheng, S. Kopta, R. C. Stevens, *J. Am. Chem. Soc.* **2001**, *123*, 3205 – 3213; b) D. L. Gin, W. Q. Gu, B. A. Pindzola, W. J. Zhou, *Acc. Chem. Res.* **2001**, *34*, 973 – 980; c) A. Mueller, D. F. O′Brein, *Chem. Rev.* **2002**, *102*, 727 – 757.
[8] a) S. Gao, B. Zou, L. F. Chi, H. Fuchs, J. Q. Sun, X. Zhang, J. C. Shen, *Chem. Commun.* **2000**, 1273 – 1274; b) B. Zou, L. Y. Wang, T. Wu, X. Y. Zhao, L. X. Wu, X. Zhang, *Langmuir* **2001**, *17*, 3682 – 3688; c) B. Zou, M. F. Wang, D. L. Qiu, X. Zhang, L. F. Chi, H. Fuchs, *Chem. Commun.* **2002**, 1008 – 1009; d) B. Zou, D. L. Qiu, X. L. Hou, L. X. Wu, X. Zhang, L. F. Chi, H. Fuchs, *Langmuir* **2002**, *18*, 8006 – 8009.
[9] J. H. Fuhrhop, U. Liman, H. H. David, *Angew. Chem.* **1985**, *97*, 337-338; *Angew. Chem. Int. Ed. Engl.* **1985**, *24*, 339 – 340.
[10] Y. Okahata, T. Kunitake, *J. Am. Chem. Soc.* **1979**, *101*, 5231 – 5234.

Received: September 30, 2002
Revised: January 21, 2003 [F4461]

 © 2003 WILEY-VCH Verlag GmbH & Co. KGaA, Weinheim